method. Its power is necessarily limited, however, because we cannot see atoms at low resolution. The electron-density peaks will no longer be spherically symmetric because of overlap and their shapes cannot be predicted without knowing the structure. This means the atomic shape function $\psi(\mathbf{n})$ becomes structure dependent. Fortunately, this does not mean that atomic resolution is an absolute necessity and we have shown that good results can be obtained starting from 3·0 Å resolution.

This present work may be regarded as a development of Sayre's own work (Sayre, 1974) on the phase extension and refinement for rubredoxin. The improvements we have brought to it are an enormous reduction of computing time, the addition of density modification and the least-squares solution of the equations. The latter enables us to make full use of very weak and accidentally absent reflexions, which contain useful information about the distribution of atoms. Sayre had to remove these from his equations because the phases of these reflexions (the variables with which he was working) have no meaning.

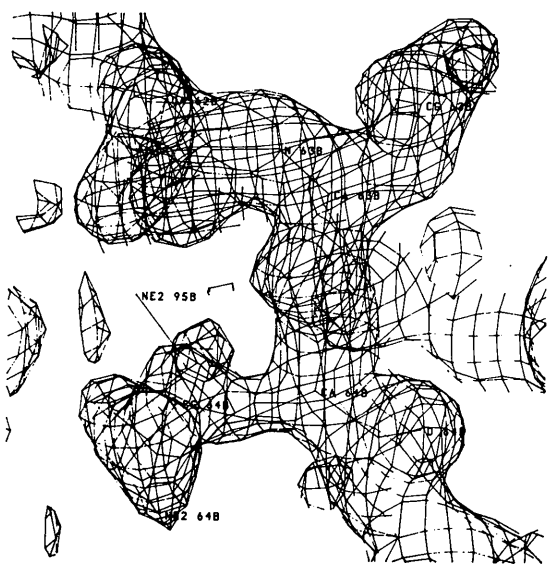


Fig. 4. Same electron density as Fig. 2 but obtained at 2 Å from the refined structure.

We wish to thank Professor G. Dodson for kindly supplying the 2Zn insulin data and atomic coordinates. We are also indebted to Mrs E. Dodson for the use of computer programs and helpful discussions. One of us (KYJZ) is grateful to the Rigaku Corporation of Japan for a research studentship, to the Dodsons for the use of their laboratory facilities and also to Professor M. M. Woolfson for encouragement and support in this project.

### References

BAKER, E. N., BLUNDELL, T. L., CUTFIELD, J. F., CUTFIELD, S. M., DODSON, E. J., DODSON, G. G., HODGKIN, D. C., HUBBARD, R. E., ISAACS, N. W., REYNOLDS, C. D., SAKABE, N. & VIJAYAN, M. (1988). *Philos. Trans. R. Soc. London Ser. B*, **319**, 369-456.

BLUNDELL, T. L., PITTS, J. E., TICKLE, I. J., WOOD, S. P. & WU, C.-W. (1981). *Proc. Natl Acad. Sci. USA*, **78**, 4175-4179.

HAUPTMAN, H. (1986). *Science*, **233**, 178-183.

KARLE, J. (1986). *Science*, **232**, 837-843.

MAIN, P. (1990). *Acta Cryst.* A**46**, 372-377.

PODJARNY, A. D., BHAT, T. N. & ZWICK, M. (1987). *Annu. Rev. Biophys. Chem.* **16**, 351-373.

RANGO, C. DE, MAUGUEN, Y., TSOUCARIS, G., DODSON, E. J., DODSON, G. G. & TAYLOR, D. J. (1985). *Acta Cryst.* A**41**, 3-17.

SAYRE, D. (1952). *Acta Cryst.* **5**, 60-65.

SAYRE, D. (1974). *Acta Cryst.* A**30**, 180-184.

WANG, B. C. (1985). *Methods Enzymol.* **115**, 90-112.

WOOLFSON, M. M. (1987). *Acta Cryst.* A**43**, 593-612.

ZHANG, K. Y. J. & MAIN, P. (1990). *Acta Cryst.* A**46**, 41-46.

*Acta Cryst.* (1990). A**46**, 381-387

# An Electron-Density Study of Germanium: Evaluation of the Available Experimental Data

BY A. S. BROWN AND M. A. SPACKMAN

*Department of Chemistry, University of New England, Armidale*, 2351 *NSW, Australia*

(*Received* 30 *May* 1989; *accepted* 5 *December* 1989)

### Abstract

Deformation and valence electron densities in germanium are derived *via* Fourier summation and multipole refinement of a selectively merged set of X-ray structure factors. The deformation density for germanium appears to be qualitatively different from that in silicon and diamond. The available experimental data are evaluated in the light of problems encountered in the electron-density analysis. In

0108-7673/90/050381-07$03.00 

particular, the uncertainties associated with the experimental measurements are compared with the valence-electron contribution to the structure factors. The need for a better and more extensive data set for germanium is highlighted.

## Introduction

The impetus for the present study was twofold. Firstly, although there have been several theoretical predictions of the electron-density distribution in germanium [see for example Wang & Klein (1981); Yin & Cohen (1982); Balbás, Rubio, Alonso, March & Borstel (1988)] and much experimental interest [see for example Matsushita & Kohra (1974); Takama & Sato (1981); and references therein] there has not been a detailed analysis of the electron-density distribution obtainable from such experimental data. Some authors [for example Matsushita & Kohra (1974); Takama & Sato (1981)] have compared experimental and theoretical scattering factors, but have not examined the resulting electron-density distributions in detail. Secondly, X-ray diffraction data can be used to obtain the electrostatic potential in the crystal using a strategy discussed in detail by Spackman & Stewart (1984). This property may be of use when considering the trapping of impurities (such as H atoms) in semiconductor materials, and is the subject of a separate paper (Brown & Spackman, 1989).

The most complete data set available in the literature is that of Matsushita & Kohra (1974; referred to as MK) collected at 293 K with Cu $K\alpha_1$ radiation, and which, apart from the absence of the 511 reflection, represents a complete sphere of reflections for $(\sin\theta)/\lambda \le 0{\cdot}5$ Å$^{-1}$. More recently, Takama & Sato (1981; referred to as TS) reported seven reflections for germanium at $\lambda = 0{\cdot}559$ Å (Ag $K\alpha_1$), apparently at room temperature, using the *Pendellösung*-beat method, including the 511 reflection necessary to complete the MK data. Mair & Barnea (1975) collected accurate X-ray data from a large single crystal, but the low-angle data in that study suffer severely from extinction and are of no use for the present study. Mair & Barnea report $F_o$ (without e.s.d.'s) for 21 reflections, all with $(\sin\theta)/\lambda > 1{\cdot}1$ Å$^{-1}$. This high-angle data would only serve to aid in the determination of $B$, the Debye–Waller factor; rather than including that data in the refinement, the value of $B$ is fixed (see below).

As noted by Takama & Sato, the excellent agreement between the TS and MK data sets depends critically on the dispersion corrections and thermal parameter used to bring the two onto a common scale. For space group $Fd3m$ with atoms at (1/8, 1/8, 1/8) the relationship between the observed structure factors, $F_o$, and the corresponding 'observed' atomic scattering factors, $f_o$, is straightforward if we assume harmonic thermal motion;

$$\begin{aligned} |F_o| &= 8|f_o| \exp[-B(\sin^2\theta)/\lambda^2] \\ &\quad \text{for } |h|+|k|+|l| = 4n, 4n+2 \\ |F_o| &= 4(2^{1/2})|f_o| \exp[-B(\sin^2\theta)/\lambda^2] \\ &\quad \text{for } |h|+|k|+|l| = 4n+1, 4n+3. \end{aligned} \tag{1}$$

Here no assumptions are made about the nature of $f_o$, except that it contains both spherical and aspherical electronic terms, and the real part of anomalous dispersion. The MK data contain contributions from only the real part of the dispersion correction, since the experiment is not sensitive to the imaginary part. The TS experiment, however, is sensitive to both the real and imaginary parts of the dispersion, $f'$ and $f''$ respectively. The data presented by TS have been corrected for the imaginary part of the dispersion (Cromer, 1965) but still contain the real part of the dispersion as well as thermal motion. Fortunately, this correction for $f''$ introduces little error, as the imaginary part of the dispersion correction is extremely well characterized, both experimentally and theoretically (Creagh, 1988). The situation for the real part, $f'$, is not as straightforward as discussed further below.

## Data reduction and analysis

An indication of the reliability of the data sets can be obtained with the following analysis. The atomic scattering factors for data collected with Ag $K\alpha_1$ and Cu $K\alpha_1$ radiation can be expressed as

$$\begin{aligned} f_{Ag} &= (f^0 + f'_{Ag}) \exp[-B(\sin^2\theta)/\lambda^2] \\ f_{Cu}/k &= (f^0 + f'_{Cu}) \exp[-B(\sin^2\theta)/\lambda^2] \end{aligned} \tag{2}$$

where $f_{Ag}, f_{Cu}$ are the experimental scattering factors, $f^0$ is the dispersion-free atomic scattering factor, $f'_{Ag}$, $f'_{Cu}$ are the real parts of the Ag and Cu dispersion corrections respectively and $k$ is a scale factor which is discussed later. Thus

$$\ln(f_{Ag} - f_{Cu}/k) = \ln(f'_{Ag} - f'_{Cu}) - B(\sin^2\theta)/\lambda^2. \tag{3}$$

A plot of $\ln(f_{Ag} - f_{Cu}/k)$ against $(\sin^2\theta)/\lambda^2$ should yield the thermal parameter, $B$, from the slope and the difference in dispersion corrections from the intercept, provided that both data sets have been collected and analysed with appropriate accuracy. Fig. 1 shows the results of this analysis applied to the six reflections common to both the MK and TS data sets. Also shown is the expected relation using the dispersion corrections of Creagh (1988) and thermal parameter from $\Theta_D = 295$ K (Ludewig, 1973). It is clearly not possible to use these data to obtain a thermal parameter which is reliable. The graph also indicates that there is a problem with one or other (or both) of the data sets, the source of which is not obvious. It is clear that the

two estimates of $|F_{111}|$ are in significant disagreement, a point noted by Takama & Sato, but not pursued by them. Given that there are no more reliable experimental data for germanium available in the literature, this electron-density analysis is necessarily compromized by the limitations of the data. However, some qualitative conclusions about the electron-density distribution do emerge, and the results may hopefully prompt the experimentalists to look again at germanium.

With only ten reflections in the data set it was necessary to employ a model with a minimum number of variable parameters. In particular, it was felt that the data were not extensive or accurate enough to refine a thermal parameter or a kappa parameter (a radial scaling factor for the valence monopole). Much care was therefore devoted to finding the best values of $B$, $\kappa$ and dispersion corrections for use in the refinement, since this necessarily meant imposing external (and therefore possibly biased) information on the refinement.

Germanium thermal parameters are most commonly reported *via* the Debye temperature, $\Theta_D$, and the relationship between $\Theta_D$ and $B$ is given exactly (Willis & Pryor, 1975):

$$B = (6h^2/mkTx^2) \times \left[(1/x)\int_0^x \{y/[\exp(y)-1]\}\,dy - (x/4)\right] \quad (4)$$
$$x = (\Theta_D/T)$$

where the symbols have their usual meanings. Ludewig (1973) has tabulated the results of several X-ray diffraction experiments from which Debye temperatures for germanium have been derived. Results

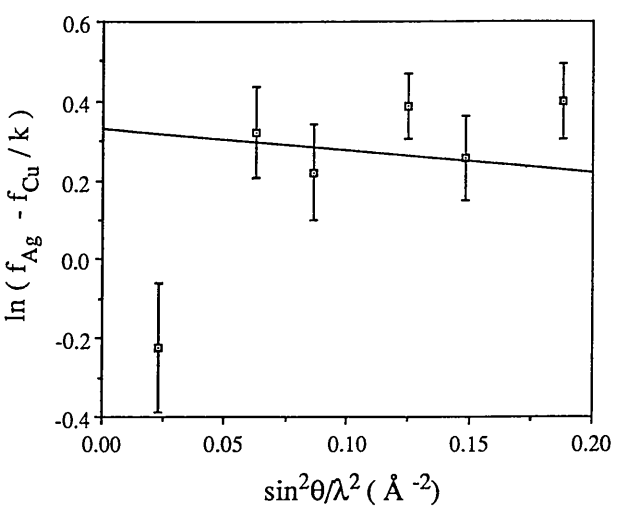


Fig. 1. $\ln(f_{Ag}-f_{Cu}/k)$ plotted against $(\sin^2\theta)/\lambda^2$ for the analysis of the reliability of MK and TS data sets (see text). The six data points are those reflections common to both data sets and the straight line is the relation expected using $B = 0{\cdot}548$ Å$^2$ (Ludewig, 1973) and $f'_{Ag}$, $f'_{Cu}$ of Creagh (1988).

in which thermal diffuse scattering and Compton scattering have been accounted for consistently yield Debye temperatures in the range 294–296 K. For $\Theta_D = 296$ K, $B = 0{\cdot}548$ Å$^2$ at $T = 293$ K. This is in excellent agreement with the value of 0·543 Å$^2$ reported by Mair & Barnea (1975) from a high-angle refinement of their data. We have made no attempt to incorporate anharmonicity in our thermal-motion model, or correct the data for this effect. Although anharmonic thermal motion in germanium has been the subject of numerous investigations (for example Roberto, Batterman & Keating, 1974; Hastings & Batterman, 1975; Mair & Barnea, 1975) corrections to $|F_o|$, as described by Spackman (1986), amount to less than $0{\cdot}5\sigma(F_o)$ for the 222 reflection and substantially less than $0{\cdot}1\sigma(F_o)$ for all other reflections. Inclusion of an anharmonicity-corrected 222 structure factor in our final data set yields no significant difference in final parameters, figures of merit or electron-density maps from those reported below. Nevertheless, future analyses of more accurate data will need to account for this effect.

The dispersion corrections used in this study are the RMP values of Creagh (1988). These were chosen because the real parts of the dispersion correction calculated by Creagh for silicon at both Mo $K\alpha_1$ and Ag $K\alpha_1$ wavelengths are in good agreement with the best experimentally determined values currently available (Deutsch & Hart, 1985). It is particularly important to use an appropriate dispersion correction with the Cu $K\alpha_1$ data, since the correction is of the order of 5% of the total scattering factor for most reflections. The dispersion corrections used in the present study were $f'_{Ag} = +0{\cdot}302$ and $f'_{Cu} = -1{\cdot}089$. The unit-cell dimension is 5·6579060 Å at 298 K (Baker & Hart, 1975).

The MK data set needs to be supplemented by the inclusion of the 511 reflection from the TS data. Inspection of the six reflections common to both data sets, corrected for dispersion and thermal motion, suggested that although both data sets purported to be absolute structure-factor measurements there appeared to be a scale difference between them. Except for the 111 reflection, the MK data were consistently smaller than the corresponding TS datum. A weighted least-squares fit was performed to scale the 511 reflection of TS to the MK data, minimizing

$$\varepsilon = \sum w(f^0_{MK}/k - f^0_{TS})^2 \quad (5)$$

where $w = \sigma^{-2}_{MK} + \sigma^{-2}_{TS}$, $f^0_{MK}$ and $f^0_{TS}$ are the dispersion- and thermal-motion-free scattering factors from MK and TS respectively, and $\sigma^2_{MK}$ and $\sigma^2_{TS}$ are the variances of $f^0_{MK}$ and $f^0_{TS}$ respectively. The least-squares fit yielded $k = 0{\cdot}9892$. Using this scale factor, dispersion corrections and thermal parameter outlined above, the scattering factor for the 511 reflection of TS, $f_{511} = 15{\cdot}61$ (17), was corrected to give an

Table 1. *Merged data set, $|F_o|$, results of pseudoatom refinement and residuals, $\Delta|F| = |F_o| - |F_c|$, after pseudoatom refinement*

Observed data are from Matsushita & Kohra (1974) unless otherwise indicated.

| *hkl* | $(\sin\theta)/\lambda$ (Å$^{-1}$) | $\lvert F_o\rvert$ | $\Delta\lvert F\rvert$ | $\Delta\lvert F\rvert/\sigma(F_o)$ |
|---|---|---|---|---|
| 111 | 0·153 | 144·74 (33)* | −0·411 | −1·244 |
| 220 | 0·250 | 173·15 (40) | +0·425 | +1·062 |
| 311 | 0·293 | 112·51 (34) | +0·186 | +0·548 |
| 222 | 0·306 | 1·05 (08) | +0·014 | +0·179 |
| 400 | 0·354 | 141·28 (42) | +0·021 | +0·050 |
| 331 | 0·385 | 95·20 (40) | +0·468 | +1·170 |
| 422 | 0·433 | 120·55 (42) | −0·133 | −0·316 |
| 333 | 0·459 | 80·51 (51) | +0·019 | +0·037 |
| 511 | 0·459 | 79·86 (87)* | −0·383 | −0·441 |
| 440 | 0·500 | 103·33 (42) | −0·431 | −1·027 |

| | | | |
|---|---|---|---|
| Scale | 0·9841 (9) | GOF | 0·90 |
| $\alpha$ (a.u.$^{-1}$) | 3·5 (fixed) | $R(F)$(%) | 0·24 |
| *O*4 | −0·20 (1) | $wR(F)$(%) | 0·26 |
| *H*9 | −0·16 (6) | $R(F^2)$(%) | 0·45 |
| $\varepsilon$ | 5·73 | $wR(F^2)$(%) | 0·52 |

* Data from Takama & Sato (1981), corrected to Cu $K\alpha_1$ dispersion and scaled by 0·9823 prior to merging (see text).

equivalent structure factor for Cu $K\alpha_1$ radiation of $F_{511} = 80{\cdot}41\ (88)$.

This data set was initially used for a multipole refinement, but proved to yield a total electron density which was significantly negative in the vicinity of the tetrahedral interstitial site [(3/8, 3/8, 3/8) and equivalent positions (labelled *T*)]. This result is not an artefact of the modelling procedure, as can be seen by the superposition of the independent atom model (IAM) electron density (obtained in direct space) and the deformation density obtained by Fourier summation of $F_o - F_{\rm IAM}$. At the *T* site the IAM electron density (atomic wavefunctions from Clementi & Roetti, 1974) is +0·03 e Å$^{-3}$, the deformation density is −0·20 e Å$^{-3}$, hence the total electron density is −0·17 e Å$^{-3}$. The e.s.d. in this quantity, estimated from $\sigma(F_o)$ values, is only 0·04 e Å$^{-3}$, making this excursion into negative, and hence non-physical, electron density highly significant. The data set must therefore be deficient in some way.

The fact that the *T* site is relatively remote from the nuclei (implying low-angle data may be suspect) and that the 111 reflection in Fig. 1 is clearly anomalous, suggested that the 111 reflection of MK be replaced by the corresponding TS datum. Repeating the scaling procedure outlined above, using only the five reflections common to both data sets, yielded $k = 0{\cdot}9823$ and Cu $K\alpha_1$ equivalent structure factors $F_{111} = 144{\cdot}74\ (34)$ and $F_{511} = 79{\cdot}86\ (87)$. This data set (Table 1) was used in the subsequent multipole refinement, and yields a total electron density positive everywhere.

The deconvolution of the electron density from its thermal motion was attempted using a rigid pseudoatom model. The description of the model follows the nomenclature of Stewart (1973, 1976). The electron density was modelled using a multipole expansion with the restriction that only monopoles, octopoles and hexadecapoles are allowed by the site symmetry of the Ge atoms in the diamond structure (Dawson, 1967). The allowed higher multipoles are represented as *o*4, *h*1 and *h*9 with variable populations *O*4, *H*1 and *H*9 respectively, with the constraint $H1 = H9$. The monopole population is constrained by the electroneutrality requirement.

Spherical atomic scattering factors for germanium were obtained from the Hartree–Fock wavefunctions of Clementi & Roetti (1974). The data set is neither extensive nor accurate enough to refine the expansion or contraction of the valence monopole *via* a kappa refinement, so all refinements have (by default) $\kappa = 1{\cdot}0$. The octopole and hexadecapole radial functions were single exponentials of the form $r^6 \exp(-\alpha_l r)$ for both higher multipoles. Initially the radial exponents of the higher multipoles were refined, with the constraint $\alpha_3 = \alpha_4\ (=\alpha)$ applied. This resulted in values of $\alpha = 4{\cdot}3\ (9)$ a.u.$^{-1}$, $O4 = -0{\cdot}17\ (12)$ and $H9 = -0{\cdot}15\ (13)$, and a correlation coefficient of 0·996 between $\alpha$ and *O*4. Although this model yields a well defined and highly significant electron distribution {provided the full covariance matrix is included when calculating $\sigma^2[\rho(\mathbf{r})]$ (Spackman & Stewart, 1984)}, it was decided to fix $\alpha$ at some standard value to remove completely this correlation between electronic parameters in the model.

A suitable value of $\alpha$ can be obtained by constraining the germanium radial function, $r^6 \exp(-\alpha r)$, to peak at approximately the same fraction of the bond length as obtained in the silicon study (Spackman, 1986). This yields $\alpha = 3{\cdot}5$ a.u.$^{-1}$, somewhat less than the optimized value discussed above, but in line with the value of 3·39 a.u.$^{-1}$ obtainable for a $4p$–$4p$ orbital product using the single-zeta atomic screening constants of Clementi & Raimondi (1963). The model thus contains three variables; scale, *O*4 and $H1 = H9$, which were optimized by minimization of

$$\varepsilon = \sum w(|F_o|^2 - |F_c|^2)^2 \qquad (6)$$

with $w = \sigma^{-2}(|F_o|^2)$, $|F_o|$ being the observed structure-factor magnitudes. The minimization procedure has been described in detail by Spackman & Stewart (1984, 1986). The nature of the stationary point reached was tested by inclusion of full second derivatives in the last cycle of least squares. The criterion for convergence described by Spackman & Stewart was satisfied for the refinement, and the e.s.d.'s reported here, both in the electron-density parameters and final electron-density maps, are from the complete inverse least-squares matrix including second derivatives. In this manner all covariances between parameters are incorporated in the calculation of $\sigma^2[\rho(\mathbf{r})]$. For the revised model with $\alpha$ fixed there

are no significant correlations between parameters in the model.

The refined variables, figures of merit, and residuals are listed in Table 1. The scale factor from the refinement is 0·9841 (9), in agreement with the proposition that the MK data are on a lower scale than the TS data. Indeed, the scale factor calculated using the five reflections common to both data sets is within 0·3% of the value obtained by the refinement. As shown in Table 1 there is no systematic trend in the residuals, $\Delta|F|$, after pseudoatom refinement. The square of the ratio $\Delta|F|/\sigma(F)$ is a good approximation to the contribution of that reflection to $\varepsilon$, and it can be seen that the 111, 220, 331 and 440 reflections between them contribute 90% of the value of $\varepsilon$. Although these reflections have $\Delta|F|$ within $1{\cdot}3\sigma(F)$, all other reflections have $\Delta|F|$ within $0{\cdot}6\sigma(F)$ and most are considerably better still. These four reflections thus represent data which are not well fitted by the pseudoatom model.

The residual electron density obtained by Fourier summation of $F_o - F_c$ is shown in Fig. 2. This map displays maximum features of 0·06 (4) e Å$^{-3}$ and minima of −0·05 (4) e Å$^{-3}$, both in the interstitial regions. The contour interval used for the residual and deformation-electron-density maps (0·025 e Å$^{-3}$) reflects the size of the e.s.d.'s derived from the experimental errors in $|F_o|$ (typically between 0·02 and 0·05 e Å$^{-3}$ at sites away from the nuclei) and facilitates interpretation of significant features in those maps. The positive features in the region between the nuclei, peaking at 0·04 (4) e Å$^{-3}$, are suggestive of bonding electron density not well fitted by the model, but these features are barely significant.

Deformation electron densities were constructed by Fourier summation using the coefficients $F_o - F_{IAM}$ (Fig. 3*a*) and $F_c - F_{IAM}$ (Fig. 3*b*) where the $F_{IAM}$ are obtained from the wavefunctions of Clementi & Roetti (1974). The deformation density obtained from the observed structure factors (Fig. 3*a*) shows an elliptical bond peak reaching a maximum of 0·18 (2) e Å$^{-3}$ at the bond midpoint. This map also displays features in the interstitial regions which have no parallels in silicon or diamond (which are isostructural with germanium). The deformation density obtained from model structure factors (Fig. 3*b*) shows similar features in the bond, with a maximum of 0·18 e Å$^{-3}$ although the contours are less elliptical in this map. There is much less structure in the interstitial regions in this map, with fairly flat minima of −0·05 e Å$^{-3}$.

The process of fitting the electron-density distribution with the multipole model provides a static map of the property of interest within the convolution approximation, provided that the thermal parameter is appropriate to the data. Fig. 4(*a*) shows the static deformation-density map derived in this way. It displays features somewhat different to the deformation Fourier maps, most obviously a bond peak with a local maximum of 0·17 (2) e Å$^{-3}$. The static valence density is mapped in Fig. 4(*b*), and is the result of the addition of the valence monopole to the static deformation-density map in Fig. 4(*a*). The valence monopole employed here derives from canonical and

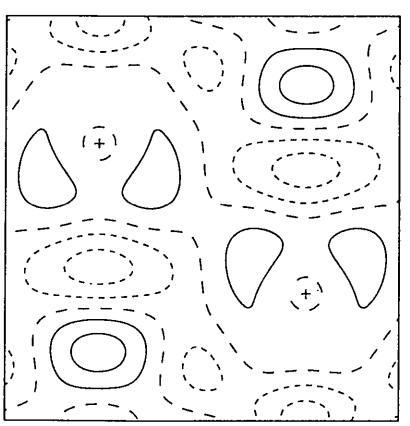

Fig. 2. Residual electron-density map after multipole refinement of the merged data set. Nuclear positions are marked with +. The contour interval is 0·025 e Å$^{-3}$ with zero and negative contours shown as dashed lines. The map is 3·8 Å horizontally (along [110]) and 3·8 Å vertically (along [001]).

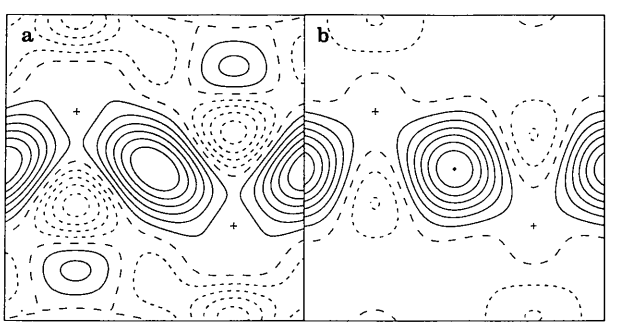


Fig. 3. Deformation electron densities, $\Delta\rho(\mathbf{r})$, obtained by Fourier summation of (*a*) $(F_o - F_{IAM})$ and (*b*) $(F_c - F_{IAM})$. Contour intervals and map dimensions are as for Fig. 2.

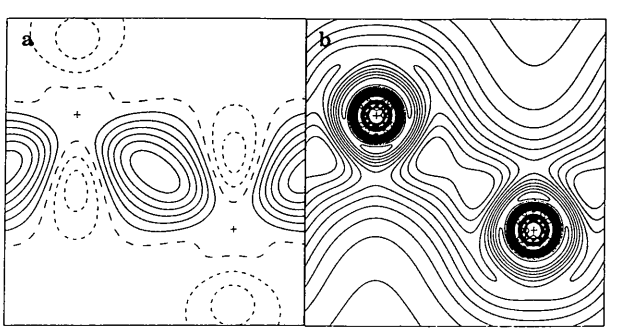


Fig. 4. (*a*) Static deformation electron density calculated from the multipole model. The contour interval is 0·025 e Å$^{-3}$; (*b*) Static valence electron density calculated from the multipole model. The contour interval is 0·05 e Å$^{-3}$. Map dimensions are as for Fig. 2.

not localized atomic orbitals, as were employed in the analysis of silicon (Spackman, 1986). As a result, there is substantial structure near the nucleus arising from the nodal behaviour of such orbitals. The main features of the map are the rectangular contours along the bond which rise to two local maxima of 0·55 (2) e $Å^{-3}$ and a saddlepoint at the bond midpoint of 0·51 (2) e $Å^{-3}$. There is no local maximum behind the atoms as occurs in silicon (Spackman, 1986).

Wang & Klein (1981) have mapped the deformation and valence electron densities for germanium from theoretical scattering factors. They obtain an elliptical bond peak in the deformation-density map with the long axis of the ellipse perpendicular to the Ge—Ge bond, rising to a maximum of 0·133 e $Å^{-3}$. This bond peak is in poor agreement with both the pseudoatom and Fourier results outlined above. The valence density reported by these authors displays some of the features shown in Fig. 4(*b*), in particular the rectangular contours along the bond which rise to a maximum of 0·463 e $Å^{-3}$, somewhat less than the present results. They note a local maximum behind and close to the atoms which is not observed in the present work. Yin & Cohen (1982) have also mapped the valence density, showing features very similar to those of Wang & Klein, except that the maximum valence density along the bond is 0·518 e $Å^{-3}$, in excellent agreement with the present work.

## Discussion

As noted in the *Introduction*, caution should be exercised in the interpretation of the various electron-density maps derived from the selectively merged data of MK and TS. Although there is generally excellent agreement between various experimental and theoretical scattering factors [see for example Takama & Sato (1981)], this tells only part of the story. The analysis of germanium is restricted firstly by the small number of reflections available. This necessarily limits the information about the electron-density distribution which may be derived from the data. The situation for germanium is, however, even worse than it may appear.

The observed structure factors may be considered as the sum of contributions from a spherical core, $F_{CORE}$, from the anomalous dispersion, $F_{DISP}$, and the remainder which is due predominantly to valence electrons, $F_{VAL}$. That is

$$F_o = F_{CORE} + F_{VAL} + F_{DISP}. \quad (7)$$

$F_{CORE}$ and $F_{DISP}$ may be readily calculated using the atomic wavefunctions of Clementi & Roetti (1974) and dispersion corrections of Creagh (1988). Although these quantities have associated *systematic* uncertainties, they are essentially free of *random* uncertainties and the *random* uncertainties inherent in $F_o$ are therefore properly associated with $F_{VAL}$. Because it is the valence-electron contribution to the structure factor which is of interest in electron-density studies, these are listed in Table 2.

Table 2. *Breakdown of contributions to $F_o$ (phased by the multipole model); $F_{CORE}$, $F_{DISP}$ and $F_{VAL}$ are on the same scale as the observed structure factors $F_o$*

Note that 333 and 511 have the same $(\sin\theta)/\lambda$, and hence $F_{CORE}$ and $F_{DISP}$ values

| *hkl* | $F_o$ | $F_{CORE}$ | $F_{DISP}$ | $F_{VAL}$ |
|---|---|---|---|---|
| 111 | −144·74 (37) | −144·30 | +5·99 | −6·43 |
| 220 | −173·15 (40) | −180·64 | +8·29 | −0·80 |
| 311 | −112·51 (34) | −119·23 | +5·79 | +0·93 |
| 222 | +1·05 (08) | 0·00 | 0·00 | +1·05 |
| 400 | −141·28 (42) | −151·22 | +8·01 | +1·93 |
| 331 | +95·20 (40) | +100·48 | −5·59 | +0·31 |
| 422 | +120·55 (42) | +128·73 | −7·74 | −0·44 |
| 333 | +80·51 (51) | +86·03 | −5·40 | −0·12 |
| 511 | +79·86 (87) | +86·03 | −5·40 | −0·77 |
| 440 | +103·33 (42) | +111·16 | −7·48 | −0·35 |

$F_{VAL}$ represents that part of the structure factor which yields information concerning the rearrangement of electron density on bonding (assuming an inert core of 28 electrons) and it is this small contribution which is modelled in the pseudoatom refinement to give the particular values of the model parameters. For all but four reflections, the valence-electron contribution to the structure factor is of similar magnitude to the e.s.d. of the observed structure factor. For the four remaining reflections, the e.s.d.'s are between 6 and 30% of the corresponding $F_{VAL}$. In the case of silicon (Spackman, 1986) the e.s.d.'s are less than 10% of the corresponding $F_{VAL}$, reflecting the much greater experimental precision for that data set. Although the e.s.d. of each reflection is only 0·2–1·0% of $F_o$ for germanium, the e.s.d. of the measurement in comparison with the valence information, $F_{VAL}$, is very poor. The multipole model has, in effect, been driven by only four reflections, and of these only two (111 and 222) have associated e.s.d.'s of less than 8%.

It would therefore be unwise to use this germanium data set for anything but the most qualitative considerations of the electron-density distribution. In particular, one must be circumspect in using the results of the multipole modelling. The interstitial maximum noted in the residual electron density (Fig. 2) reinforces the conclusion that the multipole model is unable to account correctly for the electron density in these regions of the crystal. The deformation Fourier constructed from $F_o - F_{IAM}$, however, is essentially independent of the multipole model (except for the phasing of $F_{222}$) and thus represents the best map of the deformation electron density obtainable from the merged data set. It too must be approached with a little caution since the map depends on the appropriate dispersion corrections being applied. It is obvious from Table 2 that $|F_{DISP}|$ is of the order of 4–8% of the total structure-factor

magnitude, and it is affected markedly by different dispersion corrections. For example, for the 111 reflection, applying $f'_{Cu} = -1{\cdot}31$ (Matsushita & Kohra, 1974) yields $F_{VAL} = -7{\cdot}62$, a 19% difference compared with the result in Table 2 obtained with the dispersion correction of Creagh (1988). That part of the observed structure factor which gives information about the non-spherical part of the electron-density distribution is therefore dramatically affected by the magnitude of the dispersion correction.

Within the limitations of the data, it is possible to identify qualitative deformation-density features in the interstitial regions of the crystal which, as previously noted, have no parallels in either silicon or diamond. A better data set is needed to decide whether these features are real or are an artefact of the present limited data (for example, a result of series termination or errors in one or more observations). It is envisaged that a better data set would have the following features.

Firstly, as previously noted by Dawson (1967), accurately scaled data are vital. In the present analysis the two data sets were on different scales which complicated the merging procedure and added one extra variable to the model. Secondly, even greater precision should be aimed for. Thirdly, an accurate experimental determination of the dispersion correction for the appropriate wavelength would remove some doubt from the analysis. Collection of data at a wavelength for which this correction is very small would also lessen this uncertainty. Lastly, a much more extensive data set [out to $(\sin\theta)/\lambda \geq 1{\cdot}0$ Å$^{-1}$ for example] would remove many of the difficulties encountered in the present analysis.

### References


BAKER, J. F. C. & HART, M. (1975). *Acta Cryst.* A**31**, 364-367.

BALBÁS, L. C., RUBIO, A., ALONSO, J. A., MARCH, N. H. & BORSTEL, G. (1988). *J. Phys. Chem. Solids*, **49**, 1013-1017.

BROWN, A. S. & SPACKMAN, M. A. (1989). *Chem. Phys. Lett.* **161**, 427-431.

CLEMENTI, E. & RAIMONDI, D. L. (1963). *J. Chem. Phys.* **38**, 2686-2689.

CLEMENTI, E. & ROETTI, C. (1974). *At. Data Nucl. Data Tables*, **14**, 177-478.

CREAGH, D. C. (1988). *Aust. J. Phys.* **41**, 487-501.

CROMER, D. T. (1965). *Acta Cryst.* **18**, 17-23.

DAWSON, B. (1967). *Proc. R. Soc. London Ser. A*, **298**, 395-401.

DEUTSCH, M. & HART, M. (1985). *Acta Cryst.* A**41**, 48-55.

HASTINGS, J. B. & BATTERMAN, B. W. (1975). *Phys. Rev. B*, **12**, 5580-5584.

LUDEWIG, J. (1973). *Z. Naturforsch. Teil A*, **28**, 1204-1213.

MAIR, S. L. & BARNEA, Z. (1975). *J. Phys. Soc. Jpn*, **38**, 866-869.

MATSUSHITA, T. & KOHRA, K. (1974). *Phys. Status Solidi*, **24**, 531-541.

ROBERTO, J. B., BATTERMAN, B. W. & KEATING, D. T. (1974). *Phys. Rev. B*, **9**, 2590-2599.

SPACKMAN, M. A. (1986). *Acta Cryst.* A**42**, 271-281.

SPACKMAN, M. A. & STEWART, R. F. (1984). In *Methods and Applications in Crystallographic Computing*, edited by S. R. HALL & T. ASHIDA, pp. 302-320. Oxford: Clarendon Press.

SPACKMAN, M. A. & STEWART, R. F. (1986). Unpublished paper.

STEWART, R. F. (1973). *J. Chem. Phys.* **58**, 1668-1676.

STEWART, R. F. (1976). *Acta Cryst.* A**32**, 565-574.

TAKAMA, T. & SATO, S. (1981). *Jpn. J. Appl. Phys.*, **20**, 1183-1189.

WANG, C. S. & KLEIN, B. M. (1981). *Phys. Rev. B*, **24**, 3393-3416.

WILLIS, B. T. M. & PRYOR, A. W. (1975). *Thermal Vibrations in Crystallography*. Cambridge Univ. Press.

YIN, M. T. & COHEN, M. L. (1982). *Phys. Rev. B*, **26**, 5668-5687.


*Acta Cryst.* (1990). A**46**, 387-393

# On the Quantitative Determination of Triplet Phases by X-ray Three-Beam Diffraction


BY E. WECKERT AND K. HÜMMER

*Institut für Angewandte Physik, Lehrstuhl für Kristallographie der Universität, Bismarckstrasse* 10, *D*-8520 *Erlangen, Federal Republic of Germany*


(*Received* 1 *May* 1989; *accepted* 8 *December* 1989)


### Abstract

Calculations of the integrated diffracted intensity for Renninger experiments, *i.e.* calculations of $\psi$-scan profiles scanning through three-beam positions, are reported. The fundamental equations of the dynamical theory are solved by means of an eigenvalue procedure and boundary conditions consistent with the diffraction geometry. It is shown that for non-centrosymmetric structures the three-beam $\psi$-scan profiles bear information on both the magnitude, defined in the range $0 \leq |\phi| \leq 180°$, and the sign of the triplet phase involved in the three-beam interference. In general, the $\psi$-scan profiles can be separated into two parts: a phase-dependent part ('ideal' profile) due to the interference effect and a symmetric phase-independent *Umweganregung* or *Aufhellung* profile due to the mean energy flow in a three-beam case. Both parts can be calculated by summing up the $\psi$-scan profiles for $+\phi$ and $-\phi$, one profile being reversed with respect to the three-beam point. As a result, the experimentally best suited three-beam cases for triplet phase determination should involve structure factors of nearly equal magnitude.


0108-7673/90/050387-07$03.00 